Intersite interactions in Cu L-edge XPS, XAS, and XES of doped and undoped Cu compounds

M. A. van Veenendaal and G. A. Sawatzky
Laboratory of Applied and Solid State Physics, Materials Science Centre, University of Groningen, Nijenborgh 4, 9747 AG Groningen, The Netherlands
(Received 1 October 1993)

The effect of interaction between different Cu atoms is studied by calculations on clusters with more Cu atoms for various kinds of spectroscopy, using a multiband Hubbard Hamiltonian. It is found that the inclusion of more Cu sites often leads to final states lower in energy than those that would have been found if the calculations were restricted to the Anderson-impurity limit. These effects are studied for both undoped and doped systems. These interactions are not only important for systems involving a core hole but can also be induced by the U_{dd} Coulomb interaction. Furthermore, we show that the wide shape of the main line of the Cu $2p$ XPS spectrum is not incompatible with a narrow $2p$ XES spectrum within a one-step model.

I. INTRODUCTION

Up to a few years ago high-energy spectroscopy on strongly correlated systems was usually interpreted with model systems that had as a starting point the Anderson-impurity limit.[1-7] The strong dependence of the physical properties of the high-temperature superconductors on the number of holes (electrons) in the CuO_2 planes (and also more recent similar strong doping dependences of the alkali-doped C_{60} system) led to immense theoretical research on systems containing more sites. Usually this work was done on systems thought to describe the low-energy physics, like the t-J model and the single- and triple-band Hubbard models. These systems provided a very satisfactory explanation[8,9] for the strong transfer of spectral weight from the upper Hubbard band to low-energy states observed in x-ray absorption (XAS)[10] and electron-energy-loss spectroscopy (EELS)[11] spectra as a function of hole doping. But quite often the simplifications that were necessary in order to tackle systems with many sites disabled these models for interpreting spectroscopic data. For example, to explain the total valence-band structure of CuO or the high-T_c compounds it is essential to consider all $3d$ orbitals. The inclusion of all valence orbitals strongly increases the size of the problem and in that respect it is not surprising that little work has been done so far in the study of intersite effects and doping dependencies for most high-energy spectroscopies.[12] Furthermore, usually only valence-band spectroscopies were considered. To fill this gap we have done a study on the effects of including more transition metal atoms on several high-energy spectroscopies, hereby mainly concentrating on core-level spectroscopies.

Recently we have shown[13,14] that the restriction to a single metal atom can lead to an inadequate description. As an example we considered the $2p$ XPS spectra of some late transition-metal compounds, which are in the charge-transfer regime of the Zaanen, Sawatzky, and Allen diagram.[15] In the usual interpretation in the Anderson-impurity limit the lowest $2p$ XPS final state has mainly $\underline{c}3d^{n+1}\underline{L}$ character (where $\underline{c}$ and $\underline{L}$ stand for a core hole and a ligand hole, respectively). As a result of the strong Coulomb interaction between the core hole and the valence hole, the energy of this state becomes comparable to the energy of a configuration where a charge transfer between two metal oxygen units has taken place. This leads to a $\underline{c}3d^{n+1}$ configuration for the site with the core hole and a mainly $3d^n\underline{L}$ configuration for a neighboring transition metal-oxygen unit (throughout the paper we will denote this in a convenient shorthand notation as $\underline{c}3d^{n+1};3d^n\underline{L}$, where the semicolon separates the two metal oxygen units from each other).

These intersite screening effects explain the wide asymmetric shape of the main line in CuO and the high-T_c compounds[14] (this result will be briefly recapitulated in this paper), the disappearance of this width for $NaCuO_2$, the double peaked main line of the Ni $2p$ XPS spectrum of NiO, and some of the changes in the spectrum as a result of different environments of the Ni atom.[13] We predicted[13] that these effects are also important for various other kinds of high-energy spectroscopy. Most obvious are the ones that deal with states similar to the final state of $2p$ XPS, i.e., including a core hole, like x-ray-absorption XAS and x-ray emission spectroscopy (XES). In this paper we will study these spectroscopies for CuO and the high-T_c compounds.

The paper is divided as follows. Section II will give a description of the Hamiltonian that we have used for the calculation of the spectra. The various clusters will be described throughout the rest of the text. Section III will briefly review the results for Cu $2p$ XPS. We will also discuss the effects of electron and hole doping. In Secs. IV and V the effects of intersite interactions on XAS and XES, respectively, are considered. In Sec. V we will also show that the interaction between different Cu sites is not necessarily caused by a core hole–valence hole Coulomb repulsion, but can also result from the dd-Coulomb interaction.

II. DESCRIPTION OF THE MODEL

For the calculation we have used a number of different clusters. This variety depended on the phenomenon we

wanted to describe (e.g., inclusion of apex oxygens) or was a result of restrictions imposed on the size of the clusters due to calculational effort. These clusters are all described by a similar Hamiltonian. When using a particular cluster parts of the Hamiltonian, involving orbitals not present in the cluster, will simply become zero. The total Hamiltonian is given by

$$H_{\rm tot}^{M,P}=H^{M,P}+T=H_0+H_1+H_c^{M,P}+T\ ,$$

where $H^{M,P}$ indicates whether, for the core hole part, the multiplet effects of the $2p$-$3d$ Coulomb interaction and the $2p$ spin-orbit coupling are included (H^M) or that the effect of the core hole is described by a core hole potential (H^P). H_0 describes the one-particle part of the Hamiltonian (all equations will be in hole notation):

$$\begin{aligned}H_0=&\sum_{i,\mu}\varepsilon_d d_{i,\mu}^\dagger d_{i,\mu}+\sum_{i,\gamma}E_{2p}c_{i,\gamma}^\dagger c_{i,\gamma}+\sum_{j,\nu}\varepsilon_p(\nu)p_{j,\nu}^\dagger p_{j,\nu}\\&+\sum_{i\mu,j\nu}[t_{pd}(i\mu,j\nu)d_{i,\mu}^\dagger p_{j,\nu}+\text{H.c.}]\\&+\sum_{j\nu,j'\nu'}[t_{pp}(j\nu,j'\nu')p_{j,\nu}^\dagger p_{j',\nu'}+\text{H.c.}]\ ,\end{aligned}$$

where the summations i and j go over the different metal and ligand atoms, respectively. The greek indices label the orbital and spin quantum numbers for the $3d$ (μ) and $2p$ (γ) orbitals of the transition-metal site and ν for the various oxygen $2p$ orbitals. We can divide the orbitals into two sets. First, there are the x^2-y^2 (local symmetry:b_1) and $3z^2-r^2$ (a_1) orbitals with the σ bonding O $2p$ orbitals and second, the xy (b_2) and yz,zx (e) orbitals that have a π bonding to oxygen. In order to reduce the size of the calculations, the latter set will only be included for the metal oxygen cluster with the core hole (this can still lead to matrix dimensions of a few thousand). The π-bonding oxygen orbitals are included in the appropriate symmetry around the metal site, e.g., $|p_{xy}\rangle=[|p_{y1}\rangle-|p_{y4}\rangle+|p_{x2}\rangle-|p_{x3}\rangle]/2$ or, for the apex part of p_{zx}, $|p_{zx}^{\rm apex}\rangle=[|p_{x5}\rangle-|p_{x6}\rangle]/\sqrt{2}$ (for the convention of the orbitals see Fig. 1). Although there are a large number of different hybridization matrix elements they can all be expressed in three nearest-neighbor overlap integrals (given in Slater-Koster integrals[16]): $(pd\sigma)$ and $(pd\pi)$ for transition metal-oxygen hybridization and $[(pp\pi)$-$(pp\sigma)]$ for oxygen-oxygen hopping. The values of these matrix elements are well established by band-structure calculations.[17,18] The relations between the different matrix elements follow from symmetry. We have also used Harrison's relations[19] to correct the values of the transfer integrals for the larger distance between the apex oxygen and the metal site compared to that distance in the plane. The overlap integrals scale to the power -3.5 and -2 for the pd and pp matrix elements, respectively. For the distances we have taken the values of La_2CuO_4, i.e., $d_{\rm plane}=1.89$ and $d_{\rm apex}=2.41$. More details on how to obtain the various matrix elements can be found in Ref. 20. The parameters used in the calculations are given in Table I.

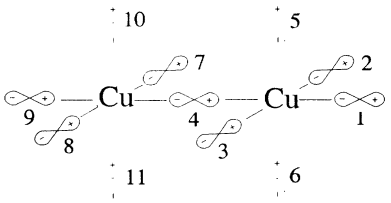

FIG. 1. The $Cu_2O_{7(11)}$ cluster used in the calculations. The O sites are numbered from 1 to 11.

The on-site dd Coulomb interaction is described by H_1,

$$H_1=\sum_{i,\mu_1,\mu_2,\mu_3,\mu_4}U_{dd}(\mu_1,\mu_2,\mu_3,\mu_4)d_{i\mu_1}^\dagger d_{i\mu_2}d_{i\mu_3}^\dagger d_{i\mu_4}\ .$$

For the clusters with the reduced basis set of x^2-y^2 and σ-bonding oxygen $2p$ orbitals, an oxygen Coulomb interaction U_{pp} is also included. Comparisons between calculations with and without oxygen Coulomb interaction showed that its effect is small.

To describe the effects of the core hole we have used two different kinds of core Hamiltonians. H^M is given for the site with the core hole as (site indices have been dropped)

$$\begin{aligned}H_c^M=&\sum_{\gamma,\gamma'}\zeta_p\langle\gamma|\boldsymbol{l}\cdot\boldsymbol{s}|\gamma'\rangle c_\gamma^\dagger c_{\gamma'}\\&+\sum_{\mu,\gamma,\mu',\gamma'}U_{pd}(\mu,\gamma,\mu',\gamma')d_\mu^\dagger d_{\mu'}c_\gamma^\dagger c_{\gamma'}\ ,\end{aligned}$$

which includes the $2p$ spin-orbit interaction and the pd Coulomb interaction with the complete multiplet structure. The values for the U_{pd} Coulomb parameters are the same as those used by Okada and Kotani.[21] The radial parts given by F_{pd}^2, G_{pd}^1, and G_{pd}^3 have been calculated within the Hartree-Fock limit[22] and were scaled down to 85% to account for atomic screening. The value used for the $2p$ spin-orbit coupling was 13.6, whereas the $3d$ spin-orbit coupling has been neglected. In other cases we will describe the effect of the core hole by a simple core hole potential (i.e., including only the monopole part of the pd-Coulomb interaction)

TABLE I. Parameter values used for the different clusters. The values for the Slater-Koster integrals refer to the in-planar matrix elements. All energies are in eV.

	Cu_3O_{10}	Cu_4O_{13}	$Cu_2O_{7(11)}$
$\varepsilon_p-\varepsilon_d$	3.5	3.5	3.5
$pd\sigma$	1.5	1.32	1.5
$pd\pi$			−0.7
$pp\sigma$	−1.0	−0.93	−1.0
$pp\pi$	0.3	0.28	0.3
A	6.5	7.36	6.5
B	0.15	0.15	0.15
C	0.58	0.58	0.58
U_{pp}	6.0	6.0	
F_{pd}^0	7.7	7.7	8.0
F_{pd}^2			7.47
G_{pd}^1			5.62
G_{pd}^3			3.20
ζ_p			13.6

$$H_c^P = F_{pd}^0 \sum_\mu d_\mu^\dagger d_\mu \langle n_c \rangle ,$$

where $\langle n_c \rangle = 0$ is no core hole is present. This procedure simplifies the calculation since it is no longer necessary to treat the core hole explicitly. The last part of the Hamiltonian

$$T = \sum_{k,\sigma} E_k a_{k,\sigma}^\dagger a_{k,\sigma} ,$$

describes the kinetic energy of an outgoing photoelectron.

Spectra have been calculated using the Lanczos method, except for the intermediate state of the XES spectrum, where an exact diagonalization is necessary to obtain the complete set of eigenvectors.

III. Cu 2p XPS

We will start with a brief recapitulation of some of the results described in our previous papers[13,14] on 2p XPS, since the aspects found for 2p XPS will return in the remainder of the paper. The 2p XPS spectrum has a large satellite structure. It is well known[3] that this is a result of the nonzero overlap of the ground with a core electron removed and the satellite wave function which has mainly $3d^9$ character. Some aspects, however, remained unclear. First, there was the wide shape of the main line which was difficult to explain within the Anderson-impurity limit. The effect of the oxygen bandwidth is canceled out by the effect that the core hole tends to skew the spectral weight towards the top of the oxygen band.[14] Second, when using Cu 2p XPS as a means of estimating valence-band parameters this often led to low values of the charge-transfer energy. In a previous paper we showed that these problems can be resolved by including more Cu atoms.[14]

The Cu 2p XPS spectrum will be described using a Cu_3O_{10} cluster [see the inset of Fig. 2(a), including only the $3d_{x^2-y^2}$ and σ-bonding O 2p orbitals]. Since the number of valence holes is unchanged in 2p XPS, this reduced basis set gives an adequate description[14] (neglecting the multiplet effects for the moment). The spectral intensity of the outgoing photoelectrons with energy E_k using an excitation radiation ω_{ex} is calculated from

$$I(E_k) \sim \mathrm{Im}\left[\left\langle E_0(N) \left| V^\dagger \frac{1}{E_0(N)+\omega_{ex}-E_k-H^P-i0^\dagger} V \right| E_0(N) \right\rangle \right] ,$$

with V describing the emission of a Cu 2p electron,

$$V = \sum_{k,\gamma} a_k c_\gamma^\dagger ,$$

where a_k creates an outgoing photoelectron with energy E_k and the same spin as the core electron.

The spectra will be displayed on a binding energy scale as is common practice for photoelectron spectroscopy. The spectra for the Cu_3O_{10} cluster with three holes is shown in Fig. 2(a). The nonlocal contribution appears at the low binding energy side of the main line. The CuO_4 unit with the core hole has predominantly a $\underline{c}3d^{10}$ configuration. The hole is in the lowest final state on a neighboring CuO_4 unit. This two hole state is in a local $^1A_1$ symmetry[23] (D_{4h} space group) also known as the Zhang Rice singlet.[24] The enhanced hybridization between $d^9\underline{L}$ and $d^{10}\underline{L}^2$ compared to d^9 and $d^{10}\underline{L}$ as a result of symmetry leads to a large stabilization energy of the two-hole state. At the high binding energy side of the main line we find the state with a $\underline{c}d^{10}\underline{L}$ character for the CuO_4 unit with the core hole, which would be the lowest final state for an Anderson-impurity calculation. This calculation also yields a reasonable satellite to main intensity ratio of 0.40 when using well established valence-band parameters.[12,17,18]

For completeness we also reproduce the hole doped spectrum.[14] For the Cu_3O_{10} cluster with four holes (33% hole doping) we find a broadening of the main line which is also found experimentally. Furthermore, there is only a slight change in satellite to main intensity ratio, indicating that conclusions from the I_s/I_m intensity ratio with respect to the $d_{x^2-y^2}$ hole density are not straightforward.[25]

We also studied the effects of electron doping of the Cu 2p XPS spectrum [see Fig. 2(c)]. In this calculation the Cu 4s band has been neglected, since symmetry effects cause it to be small.[26] The calculation has been done for a CuO_4O_{13} cluster [see the inset of Fig. 2(c) with three holes, i.e., 25% electron doping]. The core hole is created on one of the middle Cu atoms. We used a somewhat modified parameter set, which we think is more appropriate for comparing the calculation with the Cu 2p XPS spectra of the Nd-Ce-Cu-O series, considering the larger copper-oxygen distance and the smaller Madelung energy.[27] (Although it should be noted that the changes for the different parameter sets are relatively small.) In adjusting the transfer integrals we have made use of Harrison's relations.[19]

In Fig. 2(c) we observe a pole with a large spectral weight at the low binding energy side of the spectrum. Investigations of the hole density show this state to have mainly $3d^{10}$ characters on the CuO_4 unit with the core hole, whereas the other CuO_4 unit with the core hole, whereas the other CuO_4 units contain one hole. Thus, in the lowest final state, the screening is mainly accomplished by the "doped" electron. The remainder of the spectrum we propose to have a similar peak assignment as the undoped spectrum of Fig. 2(a), except in this case the cluster contains an extra electron that is not participating in the screening process. An important aspect of the spectrum is the large intensity of the low binding energy feature, which has almost 50% of total intensity of

the spectrum, whereas the doping is only 25%. The satellite to main intensity ratio is only 0.25. Therefore it should be noted that the Cu $2p$ XPS spectrum of $Nd_{2-x}Ce_xCuO_4$ cannot be simply interpreted[28,29] as a linear superposition with electron doping of the Cu $2p$ XPS spectra of CuO and Cu_2O, since this would give an intensity of the low binding energy feature (interpreted in that case as a "Cu^{1+}" site) of only 25%. Furthermore this calculation leads to the conclusion that the relatively small low binding energy feature of the Cu $2p$ XPS spectra of the Nd-Ce-Cu-O series[28,29] seems to indicate that the actual electron doping in these compounds is lower than would be expected from the amount of cerium doping. This idea is supported by other papers using chemical analysis[30,31] and transport measurements[32] that show that the cerium doping could very well lead to an excess of oxygen. Another explanation for the relatively small change between spectra of undoped and doped compounds of the Nd-series is that the extra electrons are bound to impurities preventing them from participating in the screening of the core hole.

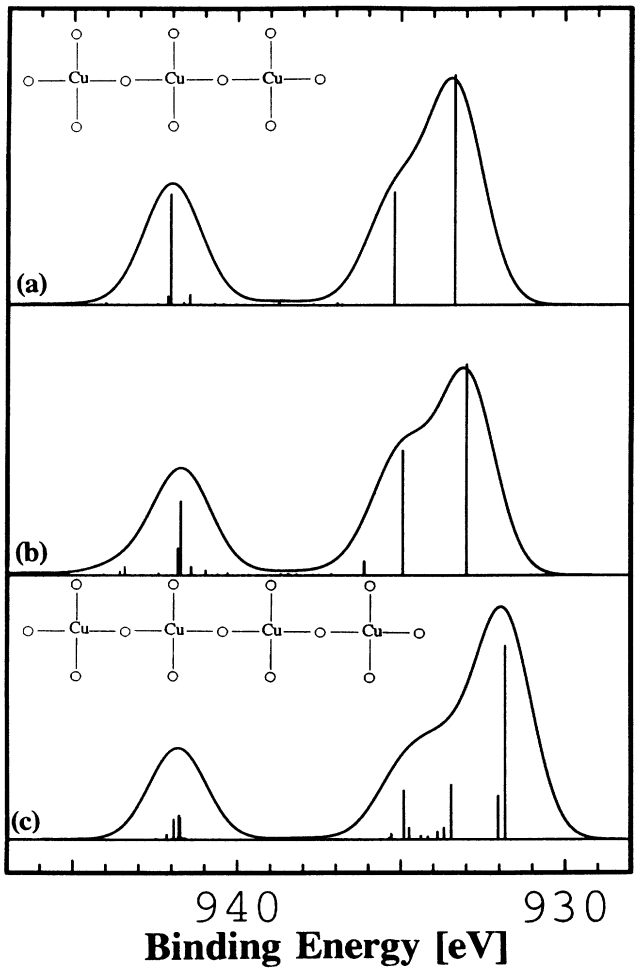

FIG. 2. Calculations of the Cu $2p$ XPS spectrum as a function of doping. (a) Cu $2p$ XPS for the Cu_3O_{10} cluster, see inset, with three holes (undoped). (b) Cu $2p$ XPS for the Cu_3O_{10} cluster with four holes (33% hole doping). (c) Cu $2p$ XPS for the Cu_4O_{13}, see inset, cluster with three holes (25% electron doping).

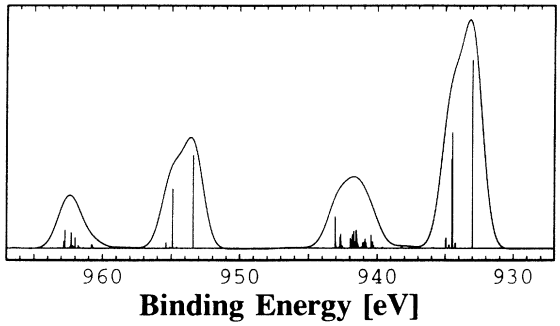

FIG. 3. Calculation for the Cu_2O_7 cluster including multiplet effects and $2p$ spin-orbit coupling.

In the remainder of the paper we will mainly use the $Cu_2O_{7(11)}$ cluster [see Fig. (1)]. This cluster includes the x^2-y^2 and the $3z^2-r^2$ orbitals and all the σ bonding O $2p$ orbitals. The $3d$ orbitals with b_2 and e symmetry and their related π bonding O $2p$ states are only included on the copper-oxygen cluster where the core hole is created. The cluster also enables us to study the difference between a cluster with apex oxygen (Cu_2O_{11}) and without apex oxygen (Cu_2O_7). Figure 3 shows the calculation of the Cu $2p$ XPS spectrum with two holes for the Cu_2O_7 cluster using H^M instead of H^P. We find the well-known division into $2p^{3/2}$ and $2p^{1/2}$, which shows the difference in intensity as a result of the difference in multiplicity of the $j=\frac{3}{2}$ and $j=\frac{1}{2}$ core levels. We note that the multiplet effect has little effect on the satellite to main intensity ratio [cf. also Fig. 7(a) for the calculation for the Cu_2O_7 cluster without multiplet structure]. Differences in the main line with the Cu_3O_{10} cluster are caused by the smaller effective hybridization between the $\underline{c}d^{10}$;ZR and $\underline{c}d^{10}\underline{L}$;↑ states, where ZR stands for a Zhang Rice singlet and ↑ for a CuO_4 unit with one hole (we stress here that with these notations we only indicate the major character of these states. The real eigenstates are, of course, a very complex mixture of the more than 3000 different components of the final-state basis set for two valence holes and one core hole). The effect of the core hole is mainly found in the shape of the satellite. The satellite for $2p^{3/2}$ has a broad shape whereas that of the $2p^{1/2}$ part of the spectrum is much narrower. (Introduction of a small crystal field or some minor changes in the parameter set[21,33] could increase the agreement of the satellite shape with experiment, but since other papers[21] have concentrated on the satellite structure, we would like to concentrate here on the intersite effects and have therefore maintained a consistent set of parameters.)

IV. Cu $2p$ XAS

During recent years a large number of papers have appeared studying the Cu $2p$ XAS spectrum of the high-T_c superconductors.[34–36] For convenience we have reproduced in Fig. 4 the data from Chen *et al.*[34] The samples were thin films of $La_{2-x}Sr_xCuO_4$ with the CuO_2 planes tilted with respect to the substrate. This enabled Chen *et al.* to obtain complete polarization along the c axis at

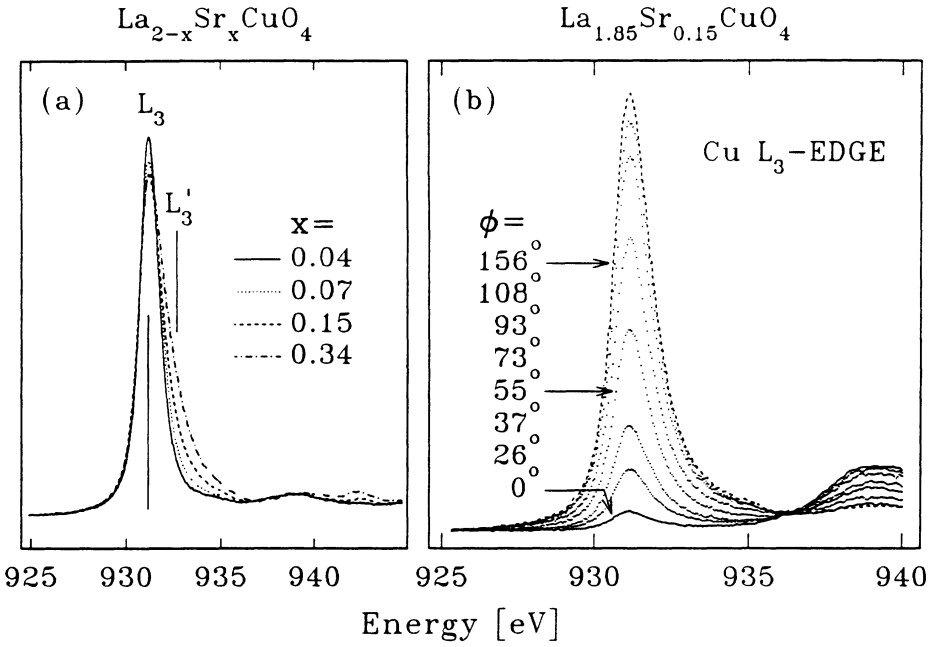

FIG. 4. L-edge fluorescence yield photoabsorption spectra, reproduced from Chen *et al.* (Ref. 34). (a) L_3-edge of $La_{2-x}Sr_xCuO_4$ for various values of x. (b) L_3-edge of $La_{1.85}Sr_{0.15}CuO_4$ for various angles, with $\mathbf{E}_h \perp c$ axis for $\phi = 156°$ and $\mathbf{E}_h \| c$ for $\phi = 0°$.

nongrazing angles. Most papers concentrated on two aspects of the spectrum. The first was the polarization dependence of the spectrum to determine the amount of $3z^2-r^2$ character of the holes in the planes [see Fig. 4(a)]. From Chen's data it can be deduced that the $3z^2-r^2$ hole density is small. However, other measurements quite often showed a larger amount of $3z^2-r^2$ character (5–10%). Second, the effects caused by hole doping were studied. Hole doping generally leads to a broadening of the white lines, indicated by L_3' in Fig. 4(b). This effect was usually interpreted[36,37] in terms of a statistical superposition of "Cu^{2+}" and "Cu^{3+}" sites. The broadening is then a result of the $d^{10}\underline{L}$ final states of the Cu^{3+} sites. However, the Cu $2p$ XAS final state of a hole doped system is very similar to the Cu $2p$ XPS final state of an undoped compound. Above (see also Refs. 13 and 14) we have shown that the XPS final state is inadequately described within the Anderson-impurity approximation. In the next paragraph we will show that the intersite effects are also important for understanding the $2p$ XAS spectrum of hole doping high-T_c compounds.

For the calculation of the Cu L-edge XAS spectrum we have used the $Cu_2O_{7(11)}$ cluster. The XAS intensity at an absorption energy of ω_{ex} is proportional to

$$I(\omega_{ex}) \sim \mathrm{Im}\left[\sum_{\alpha} \left\langle E_0(N) \left| P_\alpha^\dagger \frac{1}{E_0(N)+\omega_{ex}-H^M-i0^+} P_\alpha \right| E_0(N) \right\rangle \right] ,$$

where P_α is the dipole operator for light with polarization α,

$$P_\alpha^\dagger = \sum_{\mu,\gamma} M_\alpha(\mu,\gamma) d_\mu^\dagger c_\gamma \ .$$

The one-particle dipole matrix elements were evaluated using standard techniques.[37]

The spectrum for the undoped Cu_2O_7 cluster, i.e., for two holes in the ground state, is shown in Fig. 5(a). The spectrum shows two peaks corresponding to the L_3 and L_2 edges. The peaks are a result of a $\underline{3d}_{x^2-y^2} \rightarrow \underline{2p}_j$ transition (where $\underline{2p}_j$ stand for a core hole with $j=\frac{3}{2}$ or $\frac{1}{2}$). The L_3 and L_2 edges have the well-known branching ratio of 2:1 as a result of the different multiplicity of the $j=\frac{3}{2}$ and $\frac{1}{2}$ core levels, respectively. The satellites have little spectral weight as a result of the fact that the screening is already accomplished by the excited electron. The effect of the neighboring copper site is negligible, indicating the strongly local excitonic nature of the core hole and the excited electron. The spectrum for the undoped Cu_2O_{11} cluster is equal to that of the Cu_2O_7 within the plotting accuracy.

The XAS spectra for the $Cu_2O_{7(11)}$ clusters with three holes are shown in Figs. 5(b) and 5(c), respectively. Although a hole doping of 50% is higher than that common for most high-T_c compounds, we believe the physical effects to be very similar though somewhat less pronounced. Both spectra show as a result of hole doping extra intensity on the high-energy side of the white lines. As a result of the strong Coulomb interaction and the large stabilization energy of the Zhang Rice singlet, the character of the lowest final state is mainly $\underline{c}3d^{10}$,ZR (comparable to the lowest $2p$ XPS final of CuO). In $2p$ XPS the total valence-band spin remains the same as the ground state (i.e., $\Delta S_{\text{valence}}=0$) (neglecting the effects of $3d$ spin-orbit coupling). Therefore, of the final states with two valence holes, only the one with $S_{\text{valence}}=0$ will have

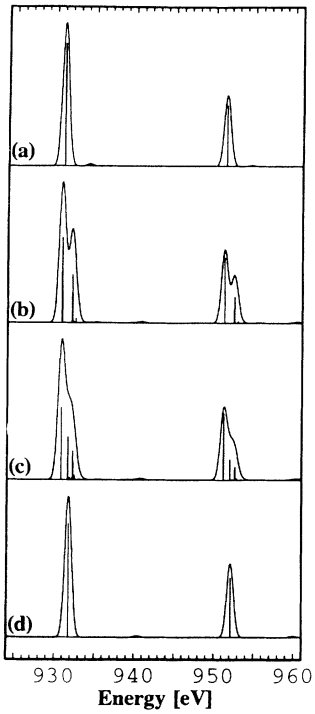

FIG. 5. Calculation of the Cu $2p$ XAS as a function of doping. (a) Cu $2p$ XAS for Cu_2O_7 cluster with two holes (undoped). (b) Cu $2p$ XAS for Cu_2O_7 cluster with three holes. (c) Cu $2p$ XAS for Cu_2O_{11} (apex oxygen) with three holes. (d) Cu $2p$ XAS for CuO_4 with two holes.

spectral weight. For $2p$ XAS however, the selection rules are $\Delta S_{\text{tot}}=0$, so the final states with the two remaining valence holes will be either in an $S_{\text{valence}}=0$ or an $S_{\text{valence}}=1$ state, yielding to an $S_{\text{tot}}=1/2$ state including the core hole, thereby leaving the total spin unchanged from the ground state.

The shoulder at high binding energy can be shown to be of triplet character. Investigations of the hole densities show this state to have a large amount of $\underline{c}3d^{10}\underline{L}_{x^2-y^2};\uparrow$ character. This state mixes with a $\underline{c}3d^{10};2$ hole($^3B_1$) configuration. Since the two-hole state with a $^3B_1$ local symmetry is at an higher energy compared to the two-hole $^1A_1$ state, the Zhang Rice singlet, the intersite effects for the triplet states are much smaller compared to the lowest final state. Note that the $^3B_1$ state also has a considerable amount of $3z^2-r^2$ character. In the ground state the $3z^2-r^2$ hole density is very small. Thus the excitation of a $2p$ electron into a $3d_{x^2-y^2}$ hole leads to $3z^2-r^2$ hole density on a neighboring $CuO_{4(6)}$ unit for these final states. We also note that the lowest singlet state with a character corresponding to the lowest final state within the Anderson-impurity limit, i.e., $\underline{c}3d^{10}\underline{L}_{x^2-y^2};\uparrow$ (thus without involving neighboring sites) has almost no spectral weight.

Upon adding apex oxygen to the cluster we observe that the broadening becomes smaller [see Figs. 5(b) and 5(c)]. This is a consequence of the fact that the two-hole $^3B_1$ state is stabilized compared to the two-hole $^1A_1$ state[20] as a result of the apex oxygen. Note that this would not happen if one disregarded nonlocal effects. In that case the high-energy final state would have mainly $3d^{10}\underline{L}_{x^2-y^2};\uparrow$ character and the effect of apex oxygen would be very small.

For formally trivalent copper compounds, like $NaCuO_2$, nonlocal screening effects are expected to be small, as we have demonstrated before for the Cu $2p$ XPS spectrum.[14] The reason for this is that an intersite charge transfer would lead to a three-hole state on a $CuO_{4(6)}$ unit, which is high in energy. This is especially so since the three-hole state also has to involve orbitals other than x^2-y^2 that have less benefit from the hybridization with oxygen (the lowest electron removal state has $^2A_1$ character[38]). Similar arguments also explain the existence of the insulating gap.[38] Therefore a calculation for a CuO_4 cluster is expected to provide an adequate description, see Fig. 5(d). We observe that the spectrum is very similar to the spectrum of the formally divalent Cu compound of Fig. 5(a), except for a shift to higher energy. (Note that we have maintained the same parameter set throughout and that we have made no special attempts to adjust the parameters for $NaCuO_2$). The white lines occur at an energy $E_F(N+1;\underline{c})-E_0(N)$. This energy difference between divalent and trivalent copper is mainly a result of the final-state energies. For the divalent Cu these have mainly $\underline{c}3d^{10}$ character, whereas for the formally trivalent Cu compound, the character is mainly $\underline{c}3d^{10}\underline{L}$. That the energy splitting is lower than the charge-transfer energy stems from the fact that the latter state benefits from hybridization with the $\underline{c}3d^9$ configuration. Finally, with regard to doping, we note that for electron doping the spectra, as a function of doping, would remain similar to that of the undoped spectrum of Fig. 5(a), so no broadening is to be expected.

In contrast to a large number of experiments, we do not find a significant intensity for z-polarized light. The contribution to the intensity of the white line is 1.1 and 2.7 % for the clusters without and with apex oxygen, respectively. To relate this to the hole densities one has to realize that the matrix elements are related to each other by

$$2|\langle p_{x,y}|P_{x,y}|d_{x^2-y^2}\rangle|=2\sqrt{3}|\langle p_{x,y}|P_{x,y}|d_{3z^2-r^2}\rangle|$$
$$=\sqrt{3}|\langle p_z|P_z|d_{3z^2-r^2}\rangle| .$$

This is a result of the low $3z^2-r^2$ hole density in the ground state (and, of course, also the low hole density in the yz and zx orbitals) that contributes to the spectrum using only P_z. The higher $3z^2-r^2$ hole density for the Cu_3O_{11} cluster comes from the fact that the presence of apex oxygen stabilizes a hole in a $3z^2-r^2$ orbital with respect to a hole in a x^2-y^2 orbital. The latter value, with apex oxygen, is in good correspondence with the low value of $2\pm0.5\%$ reported by Chen *et al.*[34] Since deviations in linear polarization, or misalignments of the crystal, and imperfections in the sample preparation only lead to higher intensities for z-polarized light, this value seems to be the most reliable. Another aspect in favor of Chen's experiments is the use of samples where the CuO_2 planes are tilted with respect to the substrate, thereby

achieving complete polarization along the c axis at nongrazing angles. Since the same final states are reached as for planar polarization, no shift of the peaks is observed, which is in agreement with Chen's data of Fig. 4(a), but in contrast to some other experiments.

V. Cu 2p XES

In a previous paper[13] we proposed that nonlocal screening effects should also be included in model calculations for x-ray emission (XES), considering the fact that the XES intermediate state is equal to the 2p XPS final state (for energies far away from threshold). During the years there has been a lot of controversy on how to deal formally with XES, especially in the treatment of the intermediate state. One can distinguish between two approaches: the one-step and the two-step models. In the latter model one assumes that the emission takes place on a fully relaxed intermediate state. In the limit of zero interaction between the core hole and the valence electrons, this state is equivalent to the initial ground state (except for the presence of the core hole). For simple metals the effect of correlations has been treated in various ways. One approach is to include the core hole in the intermediate state[39] and use the lowest energy state with the core hole present as a new ground state for the emission process. Another way of including the effect of the core hole is by multiplying the matrix elements by power-law factors[40] to account for the x-ray singularity.[41,42] In a one-step model, on the other hand, all the intermediate states are explicitly taken into account. Earlier Tanaka, Okada, and Kotani[43] treated the XES spectrum for CuO and the high-T_c compounds, using methods similar to ours. Their calculations, however, were done within the Anderson-impurity limit which gives an inadequate description of the intermediate state.

The XES spectrum for CuO and the high-T_c compounds[44] consists predominantly of a single peak at $\sim$930 eV with a width of 2–3 eV. The data by Nordgren and Wassdahl[44] have been reproduced in the inset of Fig. 6(a). The spectra were obtained using synchrotron radiation with an excitation energy of 970 eV. The data obtained with the use of synchrotron radiation should be expected to give better results as they suffer less from satellites caused by multiply ionized states. The fact that the width of the main line of the Cu 2p XPS spectrum is broader has usually been taken as a justification of the two-step model. However, band-structure calculations have shown little success in explaining the spectrum.[45] This is not surprising since correlation effects are now quite generally thought to be of importance for the description of the high-T_c compounds. Especially for the insulating compounds (and also for CuO), the relaxation time of the valence holes is expected to be long compared to the lifetime of the core hole. In that case a one-step description of the XES process is necessary. In the remainder of this section we will show that the presence of a broad main line of the Cu 2p XPS spectrum is not incompatible in the one-step model with a narrow XES spectrum.

Following a similar derivation as Gunnarsson and Schönhammer[46] in their theory on dynamical Auger theory (where the term "dynamical" refers to the fact that the dynamic screening of the core hole by valence electrons is taken into account), the outgoing x-ray photon current at an energy ω is, in the one step model, given as

$$I(\omega)\sim\sum_{\alpha}\left\langle E_0(N)\left|V^{\dagger}\frac{1}{z_0-H^P_{\rm tot}-i\Gamma}P_{\alpha}\delta(z_0-\omega-H^P_{\rm tot})P^{\dagger}_{\alpha}\frac{1}{z_0-H^P_{\rm tot}+i\Gamma}V\right|E_0(N)\right\rangle ,$$

with $z_0=E_0(N)+\omega_{\rm ex}$, and V and P_α are the 2p photoemission and the dipole operator, respectively, as used in the previous sections. The broadening term $i\Gamma$ causes a mixing of the various intermediate states, as a result of the coupling of these states via multiple Auger processes. To deal with this properly one has to describe this by a complex many-body operator. Unfortunately, as a result of the large final-state basis set, we had to neglect all interferences effects between the different intermediate states leading to the same final state, i.e., the limit $\Gamma\rightarrow 0$. However, since the most significant intermediate states have a reasonably large energy spacing compared to Γ, the interference effects are not expected to essentially alter the spectrum.

The calculation has been done for the Cu_2O_7 cluster with two holes in the ground state. For the intermediate state the Hamiltonian with the core hole potential H^P has been used. The total XES spectrum is shown in Fig. 6(a). Note that it has a similar single peaked structure as is found experimentally. The width of the peak is also smaller than that of the 2p XPS spectrum. The maximum energy of the peak is at a somewhat higher value compared to the experimental value when assuming that the 2p XPS maximum is at 933 eV [see Fig. 7(a)]. To clarify the different contributions to the spectrum a division into spectra belonging to a specific outgoing photoelectron has been made. One could denote these spectra as x-ray emission photoelectron coincidence spectra (XEPECS). The spectra shown have intermediate states with as main character $\underline{c}d^{10}$;ZR [Fig. 6(b)] and $\underline{c}d^{10}\underline{L}$;↑ [Fig. 6(c)] for the main line [poles $M1$ and $M2$ of the intermediate state spectrum shown in Fig. 7(a)], and $\underline{c}d^{9}$;↑ [Fig. 6(d)] for the satellite [pole S in Fig. 7(a)].

All the spectra have the same final states, corresponding to the final states that can be reached by photoemission. Figure 7(b) shows the 3d-electron removal spectrum for the Cu_2O_7 cluster with two holes in the ground state, comparable to a photoemission experiment done at high photon energies where the O 2p cross section is low. Some small differences with previously published spectra

by Eskes and Sawatzky[12] are a result of the somewhat simplified cluster and the neglect of the Coulomb interaction on oxygen. The states between O and 7 eV have a large amount of oxygen character, resulting from the fact that CuO and the high-T_c compounds are in the charge-transfer regime of the Zaanen, Sawatzky, and Allen diagram.[15] The satellite is a result of final states with mainly d^8 character that appear at higher energies as a result of the dd Coulomb interaction. The position of the Fermi level with respect to the final states is also indicated in the XEPECS spectra (although for this optical process the position of the Fermi level has little meaning. Note also that plotting the XES data on a binding energy scale to compare it with photoemission, as is often done, is also somewhat misleading, since it is hard to define an absolute binding energy scale considering the contributions from the different intermediate states to the total XES spectrum). The strong difference between the photoemission experiment and XES is caused by the spectral weights. For photoemission the weight for a certain final state is given by $|\langle E_F(N-1);E_k|V_{\rm PES}|E_0(N)\rangle|^2$ whereas for XEPECS for a particular intermediate state, this weight is proportional to

$$|\langle E_F(N-1);E_k|P_\omega|E_I(N-1);E_k\rangle\langle E_I(N-1);E_k|V|E_0(N)\rangle|^2 .$$

One remarkable aspect is that these spectral weights strongly depend on the intermediate state on which the emission takes place. These weights have their major contribution in a relatively small part of the final states. The energy of these final states is comparable to the energy of the intermediate states. This leads to the peaked appearance of the XES spectrum since $\omega=E_I-E_F$ will be more or less constant. The simplest way of looking at it is that the eigenstates of both initial and final states have similar phase relations except that the valence hole replaces the core hole. The $2p$ XPS satellite, which has mainly $\underline{c}d^9;\uparrow$ character, goes to $d^8;\uparrow$ after the emission process. More interesting is that the main peak of the $E_F(N-1)$ states can also be divided into two parts like the $2p$ XPS spectrum.

We see that the low binding energy feature of the Cu $2p$ XPS main line after emission predominantly ends up in the region of the final states closest to the "Fermi level." The high-energy part mainly leads to higher final-state energies. Since these latter intermediate states have mainly $\underline{c}3d^{10}\underline{L};\uparrow$ character, these final states have largely

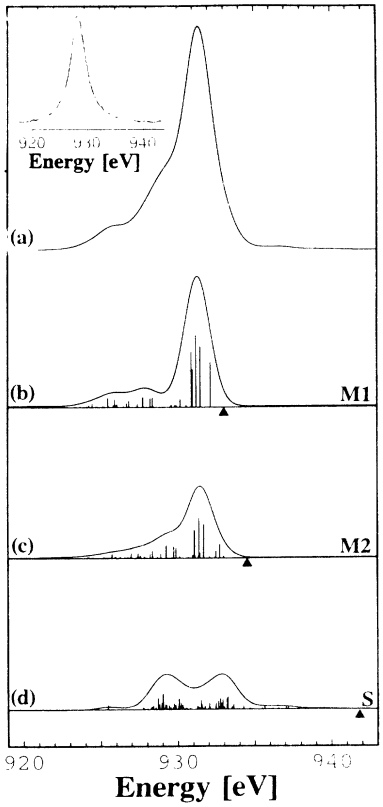

FIG. 6. Calculation of the Cu $2p$ XES spectrum. (a) total XES spectrum using the Cu_2O_7 cluster using two holes (undoped). The inset shows the experimental data as obtained by Nordgren and Wassdahl (Ref. 44). (b) XEPECS spectrum, kinetic energy corresponds to pole $M1$ of the intermediate spectrum, see Fig. 7(a). (c) The same for pole $M2$. (d) The same for the satellite (S). The arrows denote the position of the Fermi level with respect to the final states in the photoemission spectrum of Fig. 7(b).

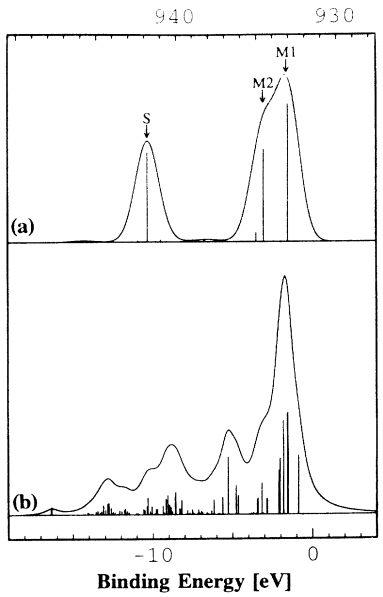

FIG. 7. Intermediate and final states of XES for the Cu_2O_7 cluster. (a) Intermediate states of Cu $2p$ XES, equivalent to Cu $2p$ XPS. $M1$, $M2$, and S denote the intermediate states used in the XEPECS calculation of Figs. 6(b), 6(c), and 6(d). (b) The $3d$ electron removal spectral function. The upper and lower binding energy scales belong to the Cu $2p$ XPS and valence-band spectrum, respectively.

two-hole (Γ);$\uparrow$ character. Γ stands here for the various final states that can be reached from an intermediate state with predominantly local b_1 symmetry. The symmetries for which the fractional parentage $\langle b_{1\uparrow} m | \} \Gamma \rangle$ is finite are $^1A_1(m=b_{1\downarrow})$, $^3B_1(a_{1\sigma})$, $^1B_1(a_{1\downarrow})$, $^3A_2(b_{2\sigma})$, $^1A_2(b_{2\downarrow})$, $^3E(e_\sigma)$, and $^1E(e_\downarrow)$.[20] On the other hand, the final states that are reached from the lowest intermediate state with mainly $\underline{c}3d^{10}$;ZR character, are γ;ZR, with local symmetry $\gamma = {}^2B_1$, $^2A_1$, $^2B_2$, and ^2E. Thus the creation of a hole by a photoemission process can lead to a final state with a Zhang-Rice singlet on a neighboring CuO_4 unit.

One could relate this effect to the kinetic effect found in Hubbard systems.[8,47,48] For hole doped Hubbard systems there are two ways of ending up in the lower Hubbard band for the electron addition spectral function. [This problem is closely related to the strong transfer of spectral weight observed in XAS (Ref. 10) and EELS (Ref. 11) experiments on doped high-T_c compounds.] First, there is the counting principle which states that for every removed electron the low-energy phase space increases by twice as much. The second effect, which further enhances the spectral weight transfer, comes from the finite transfer integral between the sites. The simplest way of looking at this effect is in lowest-order perturbation theory. In an ionic system the addition of an electron to an already occupied site would correspond to reaching a final state in the upper Hubbard band. However, after switching on the hybridization, the electron can also hop to a neighboring site which might be unoccupied, thereby contributing to the lower Hubbard band. The increase in low-energy spectral weight[47,48] is to lowest order proportional to $t\langle c^\dagger_{i\sigma} c_{j\sigma} \rangle / U$. For more complicated systems this kinetic effect is thus also possible for undoped systems.

Tanaka, Okada, and Kotani[43] found a similar explanation for the single peaked structure, also using a one-step approach, and confirm our statement that the two-step approach provides an inadequate description of the x-ray emission process. Their calculations, however, were restricted to the Anderson-impurity limit and could not satisfactorily explain the difference in widths between the Cu $2p$ XPS and XES data.

VI. CONCLUSION

In this paper we have shown that the presence of more Cu atoms often leads to final states lower in energy than those that would have been found if the calculations were restricted to the Anderson-impurity limit. For Cu $2p$ XPS they lead to the wide asymmetric main line (and also offer a transparent explanation[14] for the disappearance of this width for $NaCuO_2$). For hole doping we find similar effects as observed experimentally. It is important to note that an interpretation based on independent "Cu^{2+}" and "Cu^{3+}" sites gives a different and, in our view, incorrect insight into the physics involved. This also applied to Cu $2p$ XAS where for the broadening due to hole doping it is important whether the absorption process leads to a situation where the spin is parallel or antiparallel to the neighboring sites—an effect that could not have been found within the Anderson-impurity framework, since in that approach the neighboring transition metal sites are assumed to be of no importance.

For XES we find that the wide shape of the main line of the Cu $2p$ XPS spectrum is not incompatible with a narrower XES spectrum when using a one-step model. This presents evidence against the claim that these two effects validate the two-step model, where the emission takes place on a new "ground state" including a core hole. We also believe that for transition-metal compounds, like the ones described here, the one-step model is more appropriate since strong correlation effects will lead to long relaxation times for the intermediate state. Unfortunately, this will also severely complicate the interpretation of XES data since in the emission spectra emission from different intermediate states will be superimposed on each other.

Furthermore we have found that the inclusion of more Cu atoms is also important for the interpretation of the valence-band photoemission spectrum. Intersite effects cause a transfer of spectral weight to lower energy. The large stabilization energy of the Zhang-Rice singlet can lead to a significant spectral weight of final states with a Zhang-Rice singlet on a CuO_4 unit neighboring the Cu atom where the $3d$ electron was removed. These effects are also thought to be of importance for other models, like the degenerate Hubbard system that was proposed[49] to describe the low-energy physics in C_{60}.

ACKNOWLEDGMENTS

This work was supported by the Nederlandse Stichting voor Fundamenteel Onderzoek der Materie (FOM) and the Stichting Scheikundig Onderzoek Nederland (SON), both financially supported by the Nederlandse Organisatie voor Wetenschappelijk Onderzoek (NWO). We would like to thank Professor C. T. Chen for the use of his original data.

[1] O. Gunnarsson and K. Schönhammer, Phys. Rev. B **23**, 4315 (1983); **31**, 4815 (1985).
[2] A. Fujimori and F. Minami, Phys. Rev. B **30**, 957 (1984).
[3] G. van der Laan, C. Westra, C. Haas, and G. A. Sawatzky, Phys. Rev. B **23**, 4369 (1981).
[4] J. Zaanen, C. Westra, and G. A. Sawatzky, Phys. Rev. B **33**, 8060 (1986).
[5] A. Kotani, H. Mizuta, T. Jo, and J. C. Parlebas, Solid State Commun. **53**, 805 (1985).
[6] J. C. Fuggle, O. Gunnarsson, G. A. Sawatzky, and K. Schönhammer, Phys. Rev. B **37**, 1103 (1988).
[7] H. Ogasawara, A. Kotani, R. Potze, G. A. Sawatzky, and B. T. Thole, Phys. Rev. B **44**, 5465 (1991).
[8] H. Eskes, M. B. J. Meinders, and G. A. Sawatzky, Phys. Rev. Lett. **67**, 1035 (1991).
[9] M. S. Hybertsen, E. B. Stechel, W. M. C. Foulkes, and M.

Schlüter, Phys. Rev. B **45**, 10032 (1992).
[10]C. T. Chen, F. Sette, Y. Ma, M. S. Hybertsen, E. B. Stechel, W. M. C. Foulkes, M. Schlüter, S.-W. Cheong, A. S. Cooper, L. W. Rupp, Jr., B. Batlogg, Y. L. Soo, Z. H. Ming, A. Krol, and Y. H. Kao, Phys. Rev. Lett. **66**, 104 (1991).
[11]H. Romberg, M. Alexander, N. Nücker, P. Adelmann, and J. Fink, Phys. Rev. B **54**, 8768 (1990).
[12]H. Eskes and G. A. Sawatzky, Phys. Rev. B **43**, 119 (1991).
[13]M. A. van Veenendaal and G. A. Sawatzky, Phys. Rev. Lett. **70**, 2459 (1993).
[14]M. A. van Veenendaal, H. Eskes, and G. A. Sawatzky, Phys. Rev. B **47**, 11462 (1993).
[15]J. Zaanen, G. A. Sawatzky, and J. W. Allen, Phys. Rev. Lett. **55**, 418 (1985).
[16]J. C. Slater and G. F. Koster, Phys. Rev. **94**, 1498 (1954).
[17]A. K. McMahan, R. M. Martin, and S. Satpathy, Phys. Rev. B **38**, 6650 (1988).
[18]M. S. Hybertsen, M. Schlüter, and N. E. Christensen, Phys. Rev. B **39**, 9028 (1989).
[19]W. A. Harrison, *Electronic Structure and the Properties of Solids* (Freeman, San Francisco, 1980).
[20]H. Eskes, L. H. Tjeng, and G. A. Sawatzky, Phys. Rev. B **41**, 288 (1990).
[21]K. Okada and A. Kotani, J. Phys. Soc. Jpn. **58**, 2578 (1989).
[22]R. D. Cowan, *The Theory of Atomic Structure and Spectra* (University of California Press, Berkeley, 1981).
[23]H. Eskes and G. A. Sawatzky, Phys. Rev. Lett. **61**, 1415 (1988).
[24]F. C. Zhang and T. M. Rice, Phys. Rev. B **37**, 3759 (1988).
[25]C. N. R. Rao, G. Ranga Rao, M. K. Rajumon, and D. D. Sarma, Phys. Rev. B **42**, 1026 (1990).
[26]K. Okada, Y. Seino, and A. Kotani, J. Phys. Soc. Jpn. **59**, 2639 (1990).
[27]J. B. Torrance and R. M. Metzger, Phys. Rev. Lett. **63**, 1515 (1989).
[28]T. Suzuki, M. Nagoshi, Y. Fukuda, K. Oh-Ishi, and M. Tachiki, Phys. Rev. B **42**, 4263 (1990).
[29]H. Namatame, A. Fujimori, Y. Tokura, M. Nakamura, K. Yamachuchi, A. Misu, H. Matsubaru, S. Suga, H. Eisaki, T. Ito, H. Takagi, and S. Uchida, Phys. Rev. B **41**, 7205 (1990); A. Fujimori, Y. Toura, H. Eisaki, H. Takagi, S. Uchida, and E. Takayama-Muromachi, *ibid.* **42**, 325 (1990).
[30]E. Moran, A. I. Nazzal, T. C. Huang, and J. B. Torrance, Physica C **160**, 30 (1989).
[31]E. Wang, J.-M. Tarascon, L. H. Greene, G. W. Hull, and W. R. McKinnon, Phys. Rev. B **41**, 6582 (1990).
[32]W. Jiang, J. L. Peng, Z. Y. Li, and R. L. Greene, Phys. Rev. B **47**, 8151 (1993).
[33]M. A. van Veenendaal, G. A. Sawatzky, and W. A. Groen, Phys. Rev. B **49**, 1407 (1994).
[34]C. T. Chen, L. H. Tjeng, J. Kwo, H. L. Kao, P. Rudolf, F. Sette, and R. M. Fleming, Phys. Rev. Lett. **68**, 2543 (1992).
[35]A. Bianconi, A. Congiu Castellano, M. De Santis, P. Rudolf, P. Lagarde, A. M. Flank, and A. Marcelli, Solid State Commun. **63**, 1009 (1987); E. Pellegrin, N. Nücker, J. Fink, S. L. Molodtsov, A. Gutierrez, E. Navas, O. Strebel, Z. Hu, M. Domke, G. Kaindl, S. Uchida, Y. Nakamura, J. Markl, M. Klauda, G. Saemann-Ischenko, A. Krol, J. L. Peng, Z. Y. Li, and R. L. Greene, Phys. Rev. B **47**, 3354 (1993); M. Abbate, M. Sacchi, J. J. Wnuk, L. W. M. Scheurs, Y. S. Wang, R. Lof, and J. C. Fuggle, *ibid.* **42**, 7914 (1990); T. Takahashi, T. Kosunoki, T. Mirokawa, S. Sata, H. Katayama-Yoshida, A. Yamanaka, F. Minami, and S. Takekawa, *ibid.* **44**, 5381 (1991).
[36]K. Okada, A. Kotani, B. T. Thole, and G. A. Sawatzky, Solid State Commun. **77**, 835 (1991); D. D. Sarma, O. Strebel, C. T. Simmons, U. Neukirch, G. Kaindl, R. Hoppe, and H. P. Müller, Phys. Rev. B **37**, 9784 (1988).
[37]E. U. Condon and G. H. Shortley, *The Theory of Atomic Spectra* (University Press, Cambridge, 1935).
[38]T. Mizokawa, H. Namatame, A. Fujimori, K., Akeyama, H. Kondoh, H. Kuroda, and N. Kosugi, Phys. Rev. Lett. **67**, 1638 (1991).
[39]A. Kotani and Y. Toyozawa, J. Phys. Soc. Jpn. **35**, 1073 (1973); **35**, 1082 (1973).
[40]U. von Barth and G. Grossmann, Phys. Rev. B **25**, 5150 (1982).
[41]G. D. Mahan, Phys. Rev. B **163**, 612 (1967).
[42]P. Nozières and C. T. De Dominicis, Phys. Rev. B **178**, 1097 (1969).
[43]S. Tanaka, K. Okada, and A. Kotani, J. Phys. Soc. Jpn. **58**, 813 (1989); **60**, 3893 (1991).
[44]K.-L. Tsang, C. H. Zhang, T. A. Callcott, L. R. Canfield, D. L. Ederer, J. E. Blendell, C. W. Clark, N. Wassdahl, J. E. Rubensson, G. Bray, N. Mortensson, J. Nordgren, R. Nyholm, and S. Cramm, J. Phys. (Paris) **52**, C9-1193 (1991); J. Nordgren and N. Wassdahl, Phys. Scr. **T31**, 103 (1990); V. Barnole, J.-M. Mariot, C. F. Hague, C. Michel, and B. Raveau, Phys. Rev. B **41**, 4262 (1990).
[45]P. Marksteiner, S. Massida, J. Yu, A. J. Freeman, and J. Redinger, Phys. Rev. B **38**, 5098 (1988).
[46]O. Gunnarsson and K. Schönhammer, Phys. Rev. B **22**, 3710 (1980).
[47]A. B. Harris and R. V. Lange, Phys. Rev. **157**, 295 (1967).
[48]M. B. J. Meinders, H. Eskes, and G. A. Sawatzky, Phys. Rev. B **48**, 3916 (1993).
[49]R. W. Lof, M. A. van Veenendaal, B. Koopmans, H. T. Jonkman, and G. A. Sawatzky, Phys. Rev. Lett. **68**, 3924 (1992).